

Preparation and Characterization of Metalatranes: Alumatrane and Silatrane

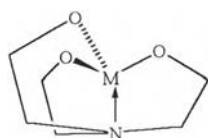
ABSTRACT

The well-developed “OOPS” or the “Oxide One Pot Synthesis” process is used for synthesizing alumatrane and silatrane directly from aluminum hydroxide (Al(OH)₃) with triisopropanolamine (TRIS) and silicone dioxide (SiO₂) with triethanolamine (TEA), respectively. Both of them uses ethylene glycol (EG) and triethylenetetramine (TETA) as a solvent and base catalyst, respectively. The process is carried out at 200°C under nitrogen atmosphere to remove EG and by-product, water. Structures of Al-TRIS and Si-TEA are characterized using TGA, FAB⁺-MS, ¹³C-NMR and FTIR. The main product of alumatrane is pentamer plus one morpholine (m/e 1250) while silatrane is the dimer plus one EG (m/e 409).

Keywords: OOPS, Alumatrane, Silatrane, Triisopropanolamine, Triethanolamine

1. INTRODUCTION

Metallatranes or simply atranes are intramolecular complex cyclic ester or alkoxides of tri(2-hydroxyalkyl)amine having a skeleton of general structure I



Structure I

M is an n-valent element connecting with inorganic or organic substituents when $n > 3$. The term metallatrane, proposed by Voronkov and Zelchan (1965), is an abbreviation used for aminotrialkoxy derivatives of different elements having the above skeleton I. For example, aminotrialkoxyphosphoranes, aminotrialkoxyboranes and aminotrialkoxysilanes give phosphanes, boratranes and silatranes,

respectively. Atrane structures are generally classified by the tricyclic model wherein a transannular M-N bond is assumed to be present.

Metallatranes with M = B, Al, Si, Ge, Sn, Pb, P, Ti, V, Mo etc. have been synthesized and studied during the last three decades (Voronkov *et al.*, 1968; Bradley *et al.*, 1978). These compounds are of interest because of their cage structure, physical/chemical properties and especially biological activity.

For synthesis of alumatrane, there are several methods to prepare alumatranes. The simplest alumatrane was prepared with high yield by the reaction of aluminum alkoxide with triethanolamine (TEA) in an aromatic solvent (benzene [Mehrotra, 1962] toluene [Thomas *et al.*, 1961]) or without solvent (Icken *et al.*, 1963; Stanley 1968; Elbing *et al.*, 1964). Triethylaluminum also reacts with TEA in toluene or hexane at -78°C to form alumatrane (Higashi and Namigawa, 1967). Verkade *et al.* (1993) used the alcoholysis of tris(dimethylamido)aluminum with TEA and also the transligation of monomeric and dimeric alumazatranes with TEA.

Laine *et al.*, (1993) found that higher boiling point amine bases (b.p. $>200^{\circ}\text{C}$), such as TEA and triethylenetetramine (TETA) could be used either in catalytic or stoichiometric quantities to dissolve SiO_2 . Moreover, they also found that approximately stoichiometric quantities of TEA will effectively dissolve $\text{Al}(\text{OH})_3$. The "Oxide One Pot Synthesis (OOPS) Process" for alkoxyalanes was developed after it was discovered that stoichiometric amount of TEA would dissolve aluminum hydroxide, the material source for most pure alumina (Kirk-Othermer, 1979; Cotton and Wilkinson, 1981).

Petchsuk *et al.* (1995) synthesized alumatrane directly from $\text{Al}(\text{OH})_3$ and TEA, and found pentamer, tetramer, trimer and the most stable species, dimer from mass spectroscopic data, ^1H -, ^{13}C - and ^{27}Al -NMR. Moreover, when TETA, a stronger base than TEA, was used, mass spectroscopic data indicated the same mixture of oligomers. Using the integral method to study the reaction kinetics, the reaction of $\text{Al}(\text{OH})_3$ and TEA is found to be a second order overall, first order with respect to $[\text{Al}(\text{OH})_3]$ and first order with respect to $[\text{TEA}]$. The activation energy for this reaction was obtained using the Arrhenius' equation and it was estimated to be 62 ± 5 $\text{kJ}\cdot\text{mol}^{-1}$. Similarly, Opornsawad *et al.* (2001) synthesized alumatrane from $\text{Al}(\text{OH})_3$

and triisopropanolamine (TRIS) via the OOPS process. Mass spectra showed that the main product was pentamer bonded with TRIS that lost one H₂O molecule. The reaction order was again second order overall, first order with respect to [Al(OH)₃] and first order with respect to [TRIS]. The activation energy of this reaction was about 24±2 kJ.mol⁻¹.

Synthesis of silatrane, pentacoordinate silicon derivative, was conducted via the reaction of trialkanolamines, such as triethanolamine with trifunctional silanes (such as RSi(OMe)₃) to yield highly crystalline, monomeric pentacoordinated silanes. The first silatrane was patented by Finestone in 1960 (Punchaipetch, 1995). Finestone suggested the existence of a Si<-N transannular coordinate bond. Silatranes are interesting because of their intriguing molecular structure, biological activity and patterns of chemical reactivity.

Punchaipetch (1995) synthesized silatrane complex directly from SiO₂ and TEA via the OOPS process. The mass spectroscopic data showed mixtures of dimer, trimer, tetramer and pentamer. The activation energy for this reaction was obtained using the Arrhenius' equation found to be 64±8 kJ.mol⁻¹. The products synthesized are tractable neutral alkoxy compounds providing novel routes to silicon containing chemical compounds, polymers, glasses and ceramics.

A parallel attempt with triisopropanolamine was unsuccessful. The silica did not dissolve and very little water was evolved even at 290°C. Verkade (1993) described similar silatrane syntheses utilizing [(RHSiO)_{2/2}]_x substrates. Silatrane could also be obtained from the reaction of trialkanolamine with appropriate polysilanes [i.e., Me (MeO)₂SiSi(OMe)₂Me] and possibly from silicon itself.

The purpose of this work is to prepare two types of metalatrane for using as a flame retardant additive in polymer blending.

2. EXPERIMENTAL

2.1 Materials

The starting materials and products are slightly moisture and air sensitive. Therefore, all operations were carried out with careful exclusion of air by cleansing with nitrogen.

UHP grade nitrogen; 99.99% purity was obtained from Thai Industrial Gases Public Co., Ltd., Thailand. Aluminum hydroxide $[\text{Al}(\text{OH})_3 \cdot x\text{H}_2\text{O}]$ and silicon dioxide (SiO_2) were purchased from Aldrich Chemical Co., Inc., USA. Triisopropanolamine (TRIS) and triethanolamine (TEA) were obtained from Fluka Chemical Co., Ltd., Switzerland and Union Carbide Co., Ltd., Thailand, respectively. All of them were used as received. Ethylene glycol (EG), used as a solvent in the reaction, was purchased from J.T. Baker Co., Ltd., USA and purified by fractional distillation at 200°C , under nitrogen prior to used. Triethylenetetramine (TETA), used as catalyst in the reaction, was obtained from Union Carbide Co., Ltd., Thailand. Acetonitrile was purchased from J.T. Baker Co., Ltd., USA and purified by standard techniques.

2.2 Instrumentation

Thermal analysis was carried out on a DuPont Thermogravimetric Analyzer (TGA). Mass spectra were obtained on a 707E-Fison Instrument with a VG data system, using in the positive fast atomic bombardment (FAB^+) mode. Carbon 13 Nuclear Magnetic Resonance (^{13}C -NMR) spectra were obtained on Bruker 300 MHz spectrometer using chloroform (CDCl_3) and tetramethylsilane (TMS) as the solvent and internal reference, respectively. Fourier Transform Infrared (FTIR) spectra were recorded on an Equinox 55 Bruker spectrometer.

2.3 Synthesis

Alumatrane was synthesized using conditions outlined by Opornsawad *et al.*, (2001). A typical synthesis was as follows:

3.55 g (45.5 mmol) of aluminum hydroxide, 13.39 g (70 mmol) of triisopropanolamine and 100 ml of ethylene glycol were added into a 250 ml two-

necked round bottle flask. The reaction mixture was stirred and heated under nitrogen in a thermostat oil bath. When the oil bath temperature reached to 200°C, the reaction was considered to commence until the reaction mixture turned clear, indicating complete reaction. Then the reaction mixture was left to stand overnight without stirring, the desired products were precipitated out and filtered. The precipitated products were stirred with acetonitrile to remove excess TRIS. The solid products were filtered off and dried under high vacuum (10^{-2} Torr) at 120°C for 5 h. NMR, FAB⁻-MS, FTIR and TGA were used to characterize the obtained products.

Silatrane was synthesized using conditions outlined by Punchaipetch (1995). A typical synthesis was as follows:

3.00 g (50 mmol) of fume silicon dioxide, 11.19 g (75 mmol) of triethanolamine, 3.65 g of triethylenetetramine (25 mmol) and 100 ml of ethylene glycol were added into a 250 ml two-necked round bottle flask. The reaction mixture was stirred and heated under nitrogen in a thermostat oil bath. When the oil bath temperature reached to 200°C, the reaction was considered to commence until the reaction mixture turned clear, indicating complete reaction. Then EG was removed by vacuum distillation (10^{-2} Torr) in a thermostat oil bath at 100°C until no more EG were removed. The precipitated products were stirred with acetonitrile to remove excess TEA. The solid products were filtered off and dried under high vacuum (10^{-2} Torr). NMR, FAB⁺-MS, FTIR, and TGA were used to characterize the dried products.

3. RESULTS and DISCUSSION

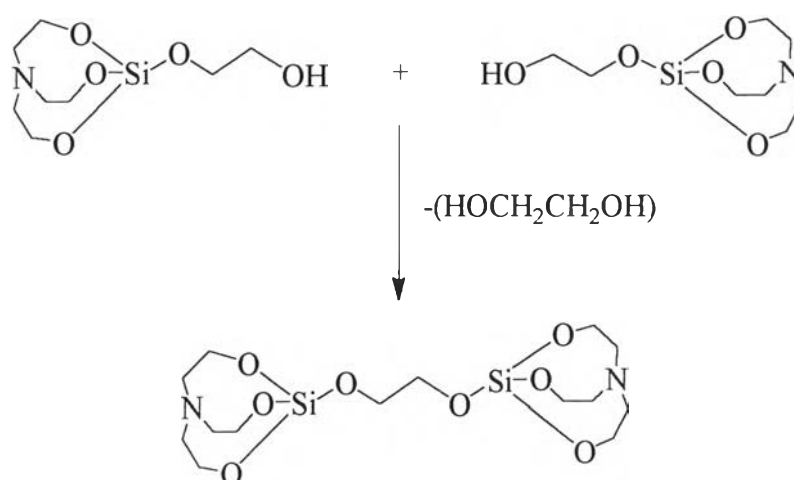
3.1 Thermogravimetric Analysis

The TGA thermogram for the alumatrane shows two major regions of weight loss (Figure 1(a)). The first small region is between 80°-230°C corresponding to the moisture desorption of alumatrane and the decomposition of excess EG and TRIS. The second major weight loss occurs in the range of 230°-650°C corresponding to the decomposition of organic ligands. The %ceramic yield of the product is 29.3% which was higher than the theoretical yield (20.4%) possibly due to a further

polymerization of alumatrane which leads to a carbon residue since the final ash is dark.

(Figure 1)

Similarly, the TGA thermogram of the silatrane (Figure 2(b)) also shows two major regions of weight loss at 130°-230°C and 230°-550°C. The first small region corresponded to the decomposition of excess EG and TEA or dimerization of (TEA)₂Si₂(EG) complexes, as shown in Scheme 1. The second major weight loss was observed due to the decomposition of organic ligands. The %ceramic yield of the product is 27.1% which is lower than the theoretical yield (29.4%). This could be the presence of TETA resulting in a lower %ceramic yield.



Scheme 1

3.2 Positive Fast Atomic Bombardment Mass Spectroscopy

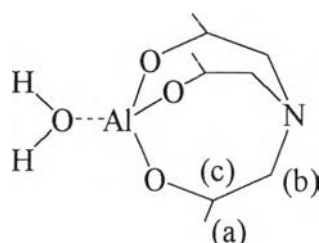
The FAB⁺ mass spectrum of alumatrane complexes implies that the product consists of two different complexes: pentamer plus one morpholine (m/e 1250) giving the highest intensity and monomer plus one TRIS (m/e 409). All proposed structures are shown in Table 1.

(Table 1)

For silatrane complexes, the FAB⁺ mass spectrum shows two different complex products. The major component is dimer plus one EG (m/e 409), the other is monomer plus one TEA (m/e 323), all proposed structures are shown in Table 2.

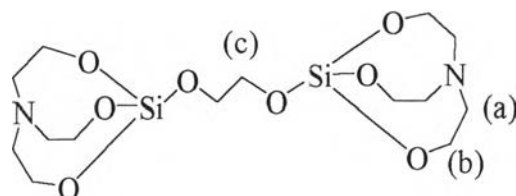
(Table 2)

3.3 Nuclear Magnetic Resonance Spectroscopy



The ^{13}C -solution NMR spectrum of the alumatrane complexes in Figure 2 shows three different resonances. The first resonance is a sharp peak at 20.0 ppm corresponding to the $-\text{CH}_3$ group at position (a). The second sharp resonance occurs at 63.5 ppm, which belongs to carbon adjacent to the nitrogen atom of TRIS at position (b). The last one is a multiple resonances at 66.0-68.0 ppm that are associated with the carbon adjacent to the oxygen atom of TRIS at position (c).

(Figure 2)



For the silatrane complexes, the ^{13}C -solid state NMR in Figure 3 also shows three different sharp resonances at 52.6, 59.0 and 64.4 ppm. These resonances can be assigned to $-\text{CH}_2\text{-N}$ of TEA at position (a), $-\text{CH}_2\text{-O}$ of TEA at position (b), and $-\text{CH}_2\text{-O}$ of EG at position (c), respectively.

(Figure 3)

3.4 Fourier Transform Infrared Spectroscopy

(Figure 4)

In Figure 4, the FTIR spectra of the alumatrane complexes show similar functional group as the spectrum of the silatrane complexes. The spectra show bands

at 3300, 2900, 1450, 1350 and 1100 cm^{-1} which can be assigned to the O-H stretching, C-H stretching, C-H bending, C-N stretching and C-O stretching, respectively. However, the spectra show the specific absorption characteristic for the alumatrane at 650 cm^{-1} corresponding to Al-O stretching and the silatrane at 1082 cm^{-1} belonging to the Si-O stretching. All assignment of both metallatranes complexes are summarized in Table 3.

(Table 3)

4. CONCLUSION

In this work, two types of metalatrane were synthesized directly from inexpensive starting materials, $\text{Al}(\text{OH})_3$ and SiO_2 , through the one step process, called "OOPS" process. Mass spectra revealed that products were oligomers. The main product of alumatrane was pentamer plus one morpholine whereas silatrane was dimer plus one EG. From TGA data, the %ceramic yields were 29.3% and 27.1% for alumatrane and silatrane, respectively.

ACKNOWLEDGEMENT

The authors would like to thank Asst. Prof. Tawan Sooknoi from King Mongkut's Institute of Technology Ladkrabang for his kind contribution in the solid state-NMR experiment.

REFERENCES

- Bradley, D.C., Mehrotra, R.C., and Gaur, D.P. (1978). Metal Alkoxides. New York: Academic Press.
- Cotton, F.A., and Wilkinson, G.F. (1981). Advanced Inorganic Chemistry. New York: Interscience Publishing.
- Elbing, I.N., and Finestone, A.B. (1964) Insulation for electrical machinery, building elements or apparatus with hardened epoxy resin. Chemical Abstract, 60(17), 4705.
- Higashi, H., and Namikawa, S. (1967). Studies on organometallic compound, ethanolamine catalyst (V): polymerization of acetaldehyde by all foil treated with HgCl_2 . Kogyo Kagaku Zasshi, 70, 97.

- Icken, J.M., and Jahren, E.J. (1963). Aluminium tris(alkoxyalkoxides) and nitrilotrialkoxides. Chemical Abstract, 60, 2768.
- Kirk-Othmer. (1979). Encyclopedia of Chemical Technology. New York: Wiley-Interscience Publishers.
- Laine, R.M., Ray, D.G., Robinson, T.R., and Viney, C. (1993). Thermotropic and lyotropic copolymers of bis(dioxyphenyl)silanes. Molecules of Crystalline Liquid Crystal, 225, 153-164.
- Mehrotra, R.C., and Mehrotra, R.K. (1962). Reaction of aluminium alkoxides with acetyl chloride. Journal of Indian Chemical Society, 39, 677.
- Opornsawad, Y., Ksapabutr, B., Wongkasemjit, S., and Laine, R.M. (2001). Formation and structure of tris(alumatranxyloxy-*t*-propyl)amine directly from Al(OH)₃ and triisopropanolamine. European Polymer Journal, 37(9), 1877-1885.
- Petchsuk, A., Dhumrongvaraporn, S., and Laine, R.M. (1995). Synthesis of Alumatrane complexes directly from Al(OH)₃ and TEA. M.S. Thesis in polymer science, The Petroleum and Petrochemical college, Chulalongkorn University, Bangkok, Thailand.
- Punchaipetch, P. (1995). Synthesis of Silatrane Complexes Directly from SiO₂ and TEA. M.S. Thesis in polymer science, The Petroleum and Petrochemical college, Chulalongkorn University, Bangkok, Thailand.
- Stanley, R.H. (1968). Water-based paints containing alkanolamine aluminate gelling agents. Chemical Abstract, 69, 78532.
- Thomas, W.M., Groszos, S.J., and Day, N.E. (1961). Alkanolamine aluminates as ester redistribution catalysts. Chemical Abstract, 55, 20966.
- Verkade, J.K. (1993). Atranans: new examples with unexpected properties. Accounts of Chemical Research, 26, 483.
- Voronkov, M.G., Seltschan, G.I. Lapsina, A., and Pestunovitsch, V.A.Z. (1968). Metalatrane (cyclic metal alcoholates of triethanolamine). Chemistry, 8., 214.
- Voronkov, M.G., and Zelchan, G.I. (1965). Preparation of organoxy (2,2',2''-nitrilotriethoxy) silanes. Khim. Geterotsikl. Soed., 51.

CAPTION OF TABLES

Table 1 The proposed structures and fragmentation of alumatrane complexes

Table 2 The proposed structures and fragmentation of silatrane complexes

Table 3 Peak position and assignments of FTIR spectra of the metalatrane complexes

CAPTION OF FIGURES

Figure 1 TGA thermogram of (a) alumatrane complexes and (b) silatrane complexes

Figure 2 ^{13}C -NMR spectrum of the alumatrane complexes

Figure 3 ^{13}C -NMR spectrum of the silatrane complexes

Figure 4 FTIR spectra of (a) alumatrane complexes and (b) silatrane complexes

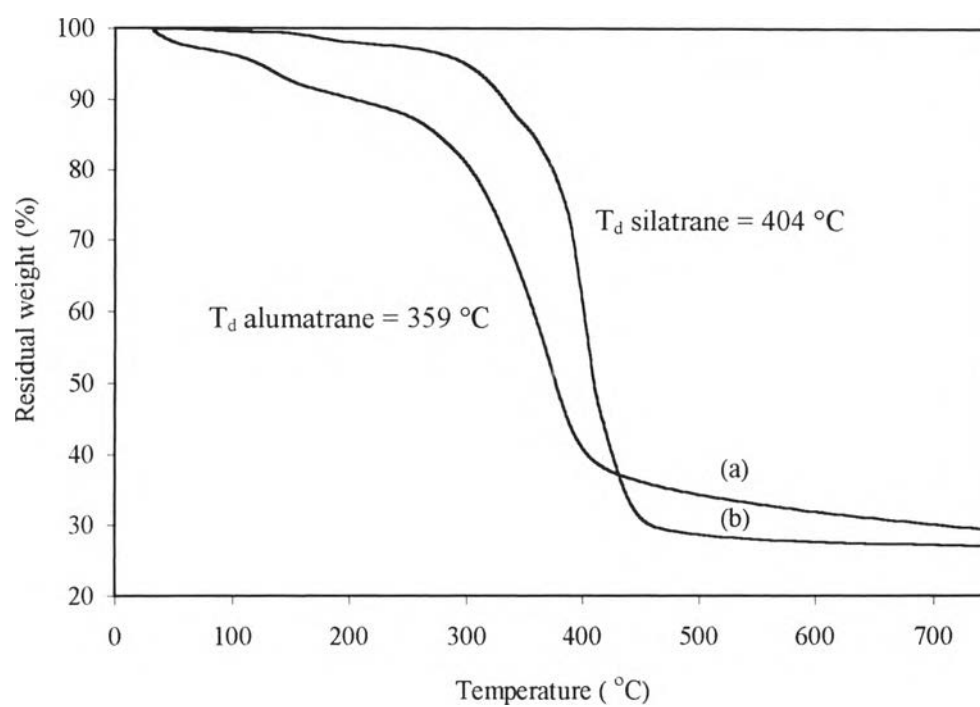
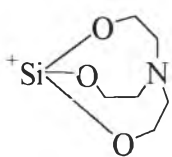
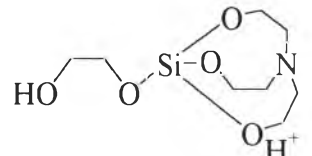
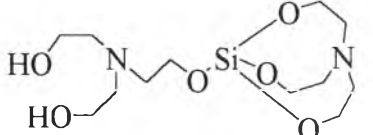
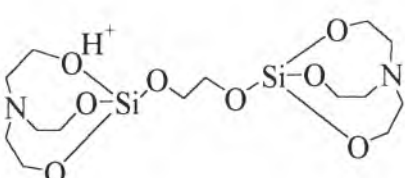


Figure 1

Table 1 The proposed structures and fragmentation of alumatrane complexes

<i>m/e</i>	Intensities	Proposed Structure
216	14.3	
409	28.6	
431	54.2	
492	37.8	
1250	100	

Table 2 The proposed structures and fragmentation of silatrane complexes

<i>m/e</i>	Intensities	Proposed Structure
174	54.2	
236	28.4	
323	36.4	
409	100	

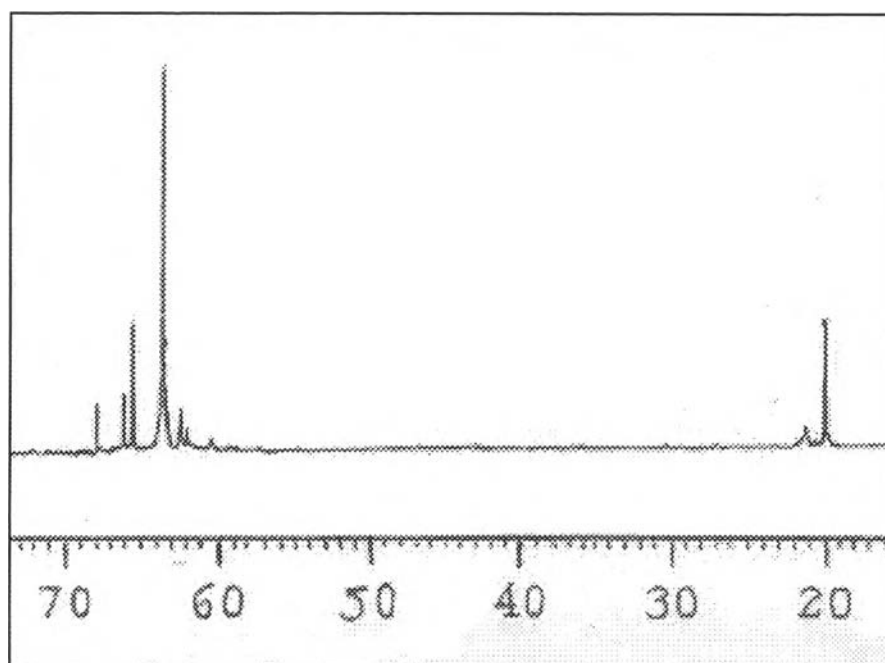


Figure 2

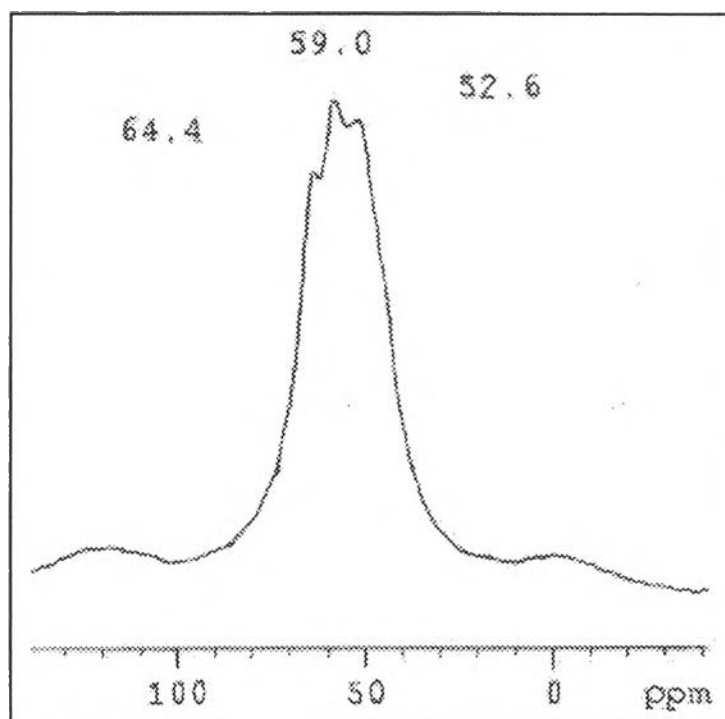


Figure 3

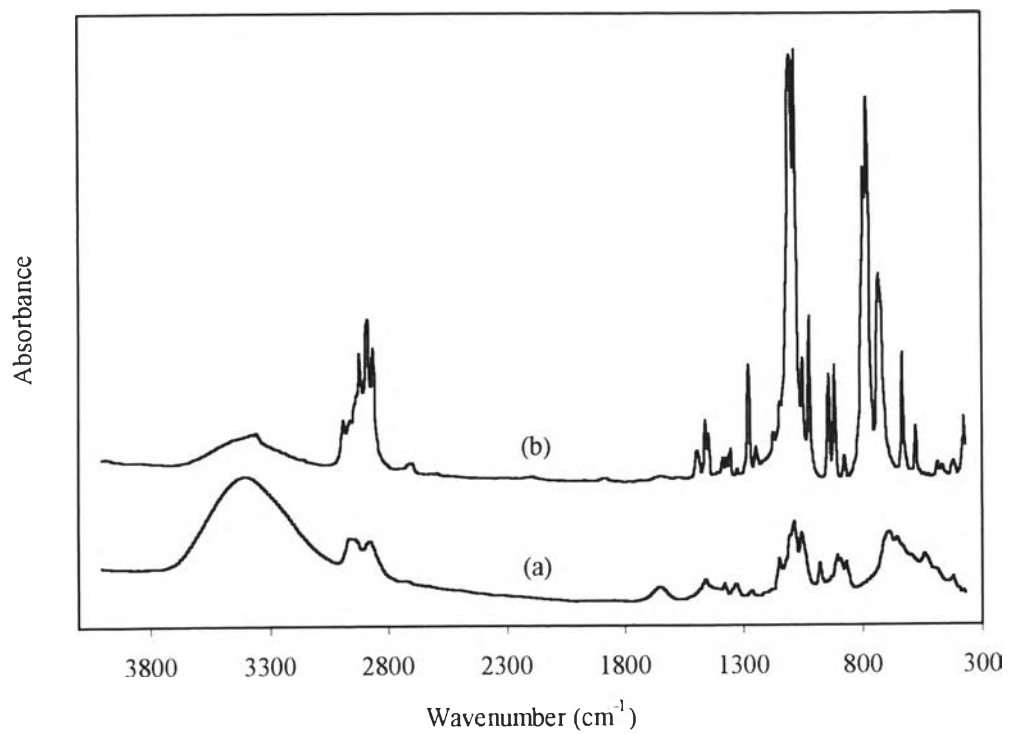


Figure 4

Table 3 Peak position and assignments of FTIR spectra of the metalatrane complexes

Assignment	Peak position of samples (cm ⁻¹)	
	Alumatrane complexes	Silatrane complexes
O-H stretching	3397	3356
C-H stretching	2960, 2875	2884
C-H bending	1458	1459
C-N stretching	1330	1274
C-O stretching	1051	1020
Si-O stretching	-	1080
Al-O stertching	650	-

Fire Retardancy of Polymer-Organoclay Nanocomposites and Polymer-Metalatrane Composites

ABSTRACT

The nanocomposites of layered silicate (based on octadecylammonium montmorillonite, OC-MMT) in commodity polymers such as Nylon 12 and PVC are prepared by melt blending. The exfoliated to partially exfoliated structures due to increasing loading are revealed by WAXD, TEM and SEM results. On the other hand, metalatrane additives (silatrane and alumatrane) melt blended with Nylon12 shows the typical composite structure according to WAXD and SEM. By TGA, water absorption and organic content in metalatrane are much higher than those in OC-MMT. As a result, at 5 wt% filler loading, the gross heat calorific values are reduced by 12.83%, 11.06%, 25.23% and 25.20% while LOI data increased to 26.8, 47.7, 26.5 and 26.4 for Nylon 12/OC-MMT, PVC/OC-MMT, Nylon 12/silatrane, and Nylon 12/alumatrane. Moreover, the mechanical properties are improved due to the rigidity of the additives; i.e. increasing tensile strength and modulus while their elongations are reduced.

Keywords: Inorganic additives, Flame retardant, Nanocomposites, Clay, Alumatrane, Silatrane

1. INTRODUCTION

Silica containing compounds are the most abundance materials in the world. With silica, materials are rather inert, strong, stiff or brittle, and the most important one is high temperature resistance. These materials are for example quartz, feldspars, sand, and clay minerals. Among several clay minerals, the layer silicates are the most useful one. Several superior properties, e.g. barrier property and reinforcement, are delivered by the incorporation of layer silicate having thickness about one nanometer in various polymeric matrices (Lan and Pinnavaia, 1994) which are now called

polymer layer silicate nanocomposites. It is believed that the two-dimensional sheet-like structure of the silicate layers can obstruct the diffusion of any mobile molecules and thus it is the key for an enhancement of barrier property (Giannelis, 1996; Messersmith, 1995) which may contribute as fire retardant by delaying the supply of oxygen and deliver of toxic combustion gases. Moreover, the fully intercalation of polymeric molecules in between silicate galleries are amazing and this can be accomplished by modifying silicate layers with organic molecules. (Yano *et al.*, 1993; Magaraphan *et al.*, 2001) Due to the molecular compatibility in nanometer range, a great reinforcement can be expected. Another silica containing compounds called silatrane is a kind of metallatrane that are recently developed (Opornsawad *et al.*, 2001). Since silatrane is from silanol modified by organic compounds, it is hydrophobic but still sensitive to water so that it can potentially be a new additive for polymers to reduce flammability.

Polymer layered silicate nanocomposites were first reported in early 1971, when Blumstein demonstrated polymerization of vinyl monomers intercalated into montmorillonite (MMT) clay. The most recent methods to prepare polymer layered silicate nanocomposites have primarily been developed by several other groups. In general these methods achieve molecular level incorporation of the layered silicate in the polymer by adding a modified silicate either to a polymerization reaction (in situ method), to a solvent-swollen polymer (solution blending), or to a polymer melt (melt blending). Additionally, one method was developed to prepare the layered silicate by polymerizing silicate precursors in the presence of a polymer (Carrado, 2000).

Two terms, viz. intercalation and exfoliation, are used to describe the two general classes of nanomorphology that can be prepared. Intercalated structures are self-assembled, well-ordered multilayered structures where the extended polymer chains are inserted into the gallery space between parallel, individual silicate layers separated by 2-3 nm. The exfoliated structures are resulted when the individual silicate layers are no longer close enough to interact with the adjacent layer's gallery cations. In the exfoliated cases the interlayer spacing can be on the order of the radius of gyration of the polymer; therefore, the silicate layers may be considered to be well dispersed in the organic polymer. The silicate layers in an exfoliated

structure may not be as well ordered as those in an intercalated structure. Both of these hybrid structures can also coexist in the polymer matrix. This nanomorphology method is very common for compositions based on smectite silicates and clay minerals.

Polymer layered silicate nanocomposites have unique properties when compared to conventional filled polymers. For example, the mechanical properties of a Nylon 6 layered silicate nanocomposites, with a silicate mass fraction only 5%, show excellent improvement over those for pure Nylon 6. The nanocomposites exhibit increase of 40% in tensile strength, 68% in tensile modulus, 60% in flexural strength and 126% in flexural modulus. The heat distortion temperature (HDT) is also increased, from 65° to 152°C and the impact strengths are lowered by just 10% (Kojima *et. al*, 1993).

The mechanical properties of aliphatic amine cured epoxy layered silicate nanocomposites, reported recently by Wang and Pinnavaia (1998), revealed an improvement of 400% or more in tensile modulus and tensile strength and a substantial increase in the strain at break. Decrease in gas permeability and increase in solvent resistance also accompany the improved physical properties (Giannelis, 1996). Additionally, polymer layered silicate nanocomposites often exhibit increased thermal stability and, as will be discussed below, reduced flammability (Burside and Giannelis, 1995).

Blumstein first reported the improved thermal stability of polymer layered silicate nanocomposites composed of polymethyl methacrylate (PMMA) and montmorillonite clay. He showed that PMMA inserted (basal spacing increase of 0.76 nm) between the lamellae of montmorillonite clay resisted thermal degradation under conditions that would otherwise completely degrade pure PMMA. These PMMA nanocomposites were prepared by free radical polymerization method. Thermogravimetric analysis (TGA) revealed that both linear PMMA and cross-linked PMMA intercalated into Na⁺ montmorillonite had a 40°-50°C higher decomposition temperature. Burside and Giannelis presented similar results in 1995 for polydimethyl siloxane (PDMS) and polyimide nanocomposites. In the case of PDMS, the nanocomposites could not be prepared by in-situ polymerization in

sodium montmorillonite, but could be carried out by melt intercalation of silanol-terminated PDMS into dimethyl ditallow ammonium treated montmorillonite. In contrast to Blumstein's case, this nanocomposite contained primarily PDMS and only 10% mass fraction of montmorillonite. Despite the low clay content, the disordered-delaminated nanostructure showed an increase of 140°C in decomposition temperature, as compared to the pure PDMS elastomer. In view of the improved barrier properties observed for other polymer nanocomposites, this increased thermal stability was attributed to hindered diffusion of volatile decomposition products within the nanocomposites. The TGA data for several aliphatic polyimide layered silicate nanocomposites also showed improved thermal stability as manifested in higher decomposition temperatures.

The first mention of potential flame retardant properties of these types of materials appeared in 1976 Japanese patent application on Nylon 6 layered silicate (montmorillonite) nanocomposites (Fujiwara and Sakamoto, 1976). However, no more studies did the serious evaluation of the flammability properties of these materials until it began in 1997 using cone calorimeter as another one parameter could determine the improved flammability behavior of a number of other polymer layered silicate nanocomposites. Gilman and Kashiwagi (1997) reported the fire retardant properties of Nylon 6 organoclay nanocomposites containing a organoclay mass fraction of only 5%. The peak heat release rate (HRR) is reduced by 63%. Furthermore, this system does not increase the carbon monoxide or soot produced during combustion. Similarly, Bourbigot, *et al.*, (2000) studied the flammability of polyamide-6/organoclay nanocomposites as textile fabrics. The result showed that the HRR is reduced by 40% in comparison with pure Nylon 6, and was lower than previous work because of preparation process of nanocomposites in which the first one was prepared via polymerization while the latter was melt blended.

In this study, to understand how the structural properties of these advanced silica containing materials influence the flammability properties of polymers, we have incorporated both materials in polyamide 12 (Nylon 12) and poly(vinyl chloride) (PVC). These two commodity polymers are used among a number of commercial products which must be flame retarded. Structural and morphological characterization of the polymer (nano)composites are revealed. The flammability

properties of these (nano)composites are then demonstrated in term of gross heat releasing, LOI, mechanical properties and general appearance. A fundamental understanding of their unique structures can be related to both physical and reduced flammability properties.

2. EXPERIMENTAL

2.1 Materials

The polyamide 12 (PA12, Nylon12), commercially available under the product name Grilamid L25 natural 6112, was supplied by EMS-Chemie (ASIA) Co., Ltd., Taiwan. The polymer is in an opaque-white pellet-bead form. The melt volume-flow rate is 20 cm³/10 min (at 275°C, load 5 kg), density is 1.01 g/cm³, and melting point is 178°C. The 258RB is the product name of a commercial polyvinyl chloride (PVC) that was supplied by VinyThai Public Co., Ltd., Thailand. The polymer is in white powder form. The viscosity index of PVC is 82 ml/g, density is 0.56 g/cm³ and melting point is 175°C. The stabilizer for PVC is Stabinex OGP-101, and was provided from Siam Stabilizers and Chemicals Co., Ltd., Thailand. The stabilizer is in white powder form, has density of 1.00 g/ml and melting point is 98°C. The stabilizer (2 phr) was mixed with PVC to increase the thermal stability of PVC during processing.

Sodium-montmorillonite (Na⁺-MMT) with cation exchange capacity (CEC) of 119 meq/100 g was supplied by Kunimine Industrial Co., Ltd., Japan. Octadecylamine used as a modifying agent was purchased from Fluka Chemical, Switzerland. The protonated agent for octadecylamine is an AR-grade hydrochloric acid (HCl) was purchased from J.T. Baker Co., Ltd., USA.

2.2 Preparation and Characterization of Si-Based Fire Retardant Additives

2.2.1 Organically Modified Montmorillonite

Na⁺-montmorillonite (Na⁺-MMT) was organically modified by ion-exchange reaction between Na⁺ and alkylammonium ion, protonated from octadecylamine

(OC). 10 Grams of Na⁻-MMT in 300 ml of distilled water was stirred overnight to swell the clay, followed by heating at 80°C for a half an hour. Separately prepared was 100 ml of 1.5 equivalent octadecylamine in 3 equivalent of HCl solution. The alkylammonium solution was gradually added into the Na⁺-MMT suspension and kept the temperature at 80°C for 2 h with vigorous stirring. Then, the product was separated and washed with 2L of hot distilled water. Filtrate was collected to determine Na⁺ ion-exchanged percentage using Varian SpectAA-300 Atomic Absorption Spectroscopy. The sediment of organically modified MMT was collected and dried overnight at 100°C. It was ground and kept in a bottle. Dried products were characterized using an Equinox 55 Bruker FTIR Spectrophotometer at frequency range 400-4000 cm⁻¹ with 16 scans, a DuPont TGA at a heating rate of 10° C/min with oxygen purge at flow rate 20 ml/min and D/MAX-2000 series of Rigaku/Wide Angle X-ray Diffractometer (WAXD) using Cu-K_α at 40kV/30mA and scanning rate of 0.02 deg/step.

2.2.2 Metalatranes

The preparation of silatrane and alumatrane followed OOPS procedure as reported by (Punchaipetch, 1995; Opornsawad *et al.*, 2001).

2.3 Preparation of Polymer-(Nano)composites

A Brabender Plasti-Corder with twin-screw extruder was used as a mixer in a melt blending technique. The polymer (Nylon12 or PVC) and organoclay (mass fraction 1, 3, 5, 7 and 9%) or metalatranes (mass fraction 5, 10, 15 and 20%) were blended in the dry-mixer for 10 min. The mixture was then fed into the hopper of the twin-screw extruder. Different temperature profile was used for different polymer (Nylon12 was 180°-185°-190°-195°C, 7 rpm and 160°-165°-170°-175°C, 15 rpm for PVC). The composite products were cooled and cut into pellets. Composite sheets were prepared by a Wabash V50H compression molding machine. The polymer nanocomposites were characterized using WAXD, SEM and TEM.

2.4 Flammability Measurements

Evaluations of flammability were achieved using the LOI tester and Bomb calorimeter. The specimen for LOI test was 6.5x70.0x3.0 mm and the sample powder was ground prior to the Bomb calorimeter test. The LOI and Bomb calorimeter tests were performed according to ASTM D 2863 and D 2015, respectively.

2.5 Mechanical Property Measurements

Investigations of mechanical properties were accomplished through the tensile, impact and hardness testing. The entire test was performed according to ASTM D 638, D 235 and D 2240 for tensile, impact and hardness test, respectively.

3. RESULTS AND DISCUSSION

3.1 Characterization of Organically Modified Montmorillonite and Metalatrane

The atomic absorption spectroscopy was used to determine the amount of Na^+ ion-exchanged with protonated octadecylamine (OC). The result shows 86.5% of Na^+ ion has exchanged, indicating that silicate surfaces are mainly covered by protonated octadecylammonium ions.

The WAXD diffractograms of Na^+ -MMT and OC-MMT are shown in Figure 1. The interlayer distance, that is basal spacing, was calculated from the peak position. The basal spacing of Na^+ -MMT is 12.01 Å at $2\theta = 7.2^\circ$, which is relatively consistent to the value reported by Yang *et al.* in 1999 (12.60 Å) and Giannelis in 1996 (11.40 Å). After modification via ion-exchange reaction, the basal spacing of OC-MMT is 26.86 Å at $2\theta = 3.2^\circ$ that is consistent with 26.91 Å reported by Thaijaroen (2000). The peak position of OC-MMT was transitioned to lower 2θ relative to Na^+ -MMT, showing that the distance between silicate layer was expanded significantly because of the incorporation of OC into MMT structure.

(Figure 1)

FTIR spectra, as shown in Figure 2, reveal the chemical group of OC, MMT and OC-MMT. All of specific peaks of OC and MMT appear in the OC-MMT spectrum implying the success of the organically modified silicate layers of MMT.

(Figure 2)

The thermogravimetric analysis was also applied to confirm the incorporation of OC into MMT structure. In Figure 3, the thermograms show the decomposition temperature (T_d) of OC, Na⁺-MMT and OC-MMT at 221°, 636° and 339°C, respectively. The improvement in T_d of modifying agent was probably due to the ionic force between alkylammonium ion and negative charge of MMT. Moreover, the heat-insulation effect of the inorganic host, silicate layers, as proposed by Lee and Jang (1997), could be partly account for the enhancement in thermal decomposition temperature of modifying agent.

(Figure 3)

The characterization of silatrane and alumatrane were already reported by Panchaipetch (1995) and Opornsawad *et al.* (2001). Both metaltranes appear as white puffy powder. It has to note here that by TGA analysis, %ceramic yields of silatrane and alumatrane are 27.1% and 29.3%, respectively with degradation temperatures (by differential values) of 404 °C and 359 °C. The initial weight loss is due to water and bound water which total content is 1% and 7% for silatrane and alumatrane. This suggests that both metaltranes have higher organic and water contents than OC-MMT. According to WAXD results, both metaltranes are not amorphous as their reactants but are the crystallite materials.

3.2 Characterization of Polymer-Organoclay and Polymer-Silatrane Composites as a Thin Film

Two kinds of polymer matrices, Nylon 12 and PVC, were used for OC-MMT and only Nylon 12 for metalatrane. In case of polymer-organoclay, they appeared in pale brown color whose hue increased with organoclay loading. For polymer-silatrane, they gave no change in color, still white.

(Figure 4)

There are no diffraction 2θ peaks between 2° and 10° in the WAXD diffractograms of Nylon 12/OC-MMT at loading of 1 and 3wt% as shown in Figure 4. This indicates that silicate layers are separated into individual layers so called exfoliated form. When the organoclay loading increased to 5wt%, small peaks appeared at 3.06° and 5.84° , corresponding to basal spacing 28.84 \AA and 15.13 \AA , respectively. When organoclay loading was increased to 7 and 9wt% both peaks appeared clearly, revealing the presence of silicate layers existing in an intercalated form, which is rather consistent to the value reported by Thajareon (2000) that the presence of a small peak also observed after loading organoclay to 7 phr.

(Figure 5)

Similarly, the WAXD diffractograms of PVC/OC-MMT (Figure 5) showed a small peak at 2.40° with an organoclay loading of 5wt% corresponding to a basal spacing of 35.87 \AA . The peak was more obvious when loading was increased to 9wt%. This exfoliated structure at low was confirmed in Figure 6, showing transmission electron micrographs of OC-MMT (5wt%) nanocomposite with (a) Nylon 12 and (b) PVC. Both of them showed partially intercalated structures owing to the concentration increase of organoclay in the polymer matrix, forming stacking of silicate layers. The aggregate formation with increasing organoclay contents is in agreement with WAXD results.

(Figure 6)

(Figure 7)

The WAXD diffractograms for the synthesized silatrane and Nylon 12/silatrane at various compositions are shown in Figure 7. For synthesized silatrane only, the WAXD pattern, e.g. small peaks at 9.64° , 10.46° , 12.36° , 13.76° , 14.22° and 15.12° corresponding to basal spacings of 7.01 \AA , 6.57 \AA , 5.76 \AA , 5.29 \AA , 5.15 \AA and 4.90 \AA respectively, reveals that silatrane is a crystallite material differing from its raw materials, amorphous silica. However, this pattern is disappeared for 5wt% silatrane in Nylon 12 and shown again at silatrane concentration of 10wt%. All peak intensities became apparent when silatrane concentration was increased to 15 and 20wt%. Since there is no change in peak positions, this simply suggests that the more silatrane content, the more its density is found in the matrix which is confirmed

by scanning electron microscopy (SEM) in Figure 8. Figure 8(a) shows good dispersion of 5wt% silatrane in Nylon12 matrix as indicated by good interfacial bonding between the additives and the bulk material, see Figure 8(e). However, according to low content, it is hardly found the silatrane particles as compared to the dispersion at higher filler content, see Figures 8(b), (c) and (d) for 10, 15 and 20wt% silatrane loading; they also show free distribution of each particle in the matrix and no aggregation of two or more particles is found. These results agree with the WAXD diffractograms that become more intense and sharper with increasing silatrane concentration. This good dispersion is attributed to high organic content that makes the filler highly hydrophobic. The particle size of silatrane at any compositions is about 300 nm, measured directly from SEM. Due to this particle dimension of silatrane, the mixed materials are thus polymer composite.

(Figure 8)

3.3 Effect of OC-MMT and Silatrane Loading on Flammability Properties

The LOI measurement of Nylon 12 and PVC with OC-MMT or silatrane are shown in Figure 9. The results obtained clearly show that LOI value increased with increasing amounts of OC-MMT or silatrane. The improvement of LOI value on Nylon 12 with OC-MMT and silatrane give similar results, i.e. LOI values of Nylon 12 increasing from 20.4 to 22.9-28.2 and 26.5-29.1 for OC-MMT and silatrane, respectively, and PVC from 35.6 to 45.2-49.0. Silatrane gradually enhances LOI values of Nylon 12 while OC-MMT is more effective; i.e. only 9wt% OC-MMT can bring about the same LOI value as silatrane of 20wt%. In case of PVC, OC-MMT shows greater enhancement of LOI and thus make PVC strongly self-extinguishable material. However, although PVC does not cause flame spreading, it is still harmful because it usually produces toxic gases, e.g. HCl as a by product of burning.

(Figure 9)

The bomb calorimeter is another method for studying the flammability of materials. It can determine the gross heat calorific values by the combustion of materials. The bomb calorimeter results are shown in Figure 10. Gross heat releasing from pure Nylon12 are about twice that of pure PVC. In other words, burning Nylon12 is more severe than PVC in term of heating to the environment.

Adding both additives in the polymers successfully reduces gross heat releasing. In case of Nylon12, the gross heat drops fast at low concentration of additives e.g. at 5wt% and gradually reduces with increasing concentrations. When comparing the two additives, silatrane is more effective to lower gross heat value than OC-MMT; i.e. only 5wt% of silatrane can bring down more heat than 9wt% OC-MMT and when adding 20wt% silatrane, the heat reduces by twice that of 9wt% OC-MMT adding. The gross heat calorific value of Nylon 12 in the Nylon 12/organoclay nanocomposites is reduced by 5.0%-14.9% and in the Nylon 12/silatrane composites by 25.2%-33.3%. In case of PVC OC-MMT can reduce the gross heat calorific value of PVC by 4.7%-13.4% which is about the same efficiency as for Nylon12. In addition, the bomb calorimeter testing allows one to detect change in pH of the combustion solution as a way to track the acidity of toxic gas releasing during combustion e.g. for our interest, HCl from burning of PVC. The combustion solution was collected from the combustion chamber. The measured pH values of the combustion solution increase from 2.15 to 2.32, 2.54, 2.82, 3.04 and 3.19 for OC-MMT concentrations of 1, 3, 5, 7 and 9wt%, respectively. These results indicate that the silicate clay layers are effectively reduced volatile toxic substances delivered during combustion from PVC nanocomposites and hence the silicate clay layers act as barrier or protective layers to retard the diffusion of toxic substances. According to the results of both LOI and gross heat values, 5wt% of the additives is effective enough to reduce flammability of the polymers.

(Figure 10)

In summary, according to fire retardant ability, polymer nanocomposites with OC-MMT show good ability as fire retardants to enhance LOI while silatrane is excellent to reduce gross heat calorific value. This suggests the different mechanisms to retard flammability of each additive besides the good heat resistant nature of these fillers. For OC-MMT, it is suggested that the silicate layers in nanocomposite structure act as a barrier to retard oxygen diffusion-in and HCl diffusion-out and its high degradation temperature (high heat resistance) causes the lowering gross heat values. In case of silatrane, it reduces LOI by its nature of high heat resistance and for excellent reduction of gross heat; the mechanism is, in addition, due to the heat use as latent heat to remove moisture and bound water out of the materials. However, this

phenomenon is not accelerated with higher content of silatrane which may be due to higher organic content in silatrane burnt off and thus giving off additional heat. This rationale also suggests the less effective to retard fire at higher loading of additives; i.e. due to additional organic content in the additives supplied to the materials. The organic part cannot withstand high temperature as inorganic part; degradation temperatures of OC-MMT and silatrane are about 300-400 °C lower than pure montmorillonite and silica. Flame temperature is believed to have higher temperature than 400 °C and thus those additional organic content will turn to be good fuel.

Another observation that simultaneously contributes to the reduced flammability is char formation. During the combustion, the char formation was appeared at the polymer surface for both fillers and at any filler composites, see Figure 11.

(Figure 11)

Visual observation of combustion experiments in the LOI tests reveals different behavior for the Nylon 12 and PVC/organoclay nanocomposites and Nylon 12/silatrane composites, compared to the pure Nylon 12 and PVC from the beginning of the thermal exposure. In the case of pure Nylon 12 and PVC, this char layer fractures into small pieces at the early stage of the combustion whereas the char does not fracture in case of the organoclay nanocomposites of Nylon 12 and PVC and Nylon 12/silatrane composites. This tougher char layer survives and grows throughout the combustion, yielding a rigid char brick with the same dimensions as the original sample, see Figure 12. This is characteristic of a material that forms a char layer during combustion (Gilman and Kashiwagi, 1997). The char formation reduces the amount of small, volatile polymer pyrolysis fragments or flammable fuels to burning in the gas phase; this in turn reduces the amount of gross heat calorific value and is fed back to polymer surface (Messersmith and Giannelis, 1995). The char insulates the underlying polymer, due to its low thermal conductivity or thermal diffusivity, and reradiate incident energy away from the polymer surface (Kashiwagi *et al.*, 1999). The char also functions as a mass transport barrier, by physically delaying the volatilization of decomposition products, causing the high LOI value (Bolf *et al.*, 1999). Moreover, the transport rate of the

thermal degradation products can be reduced by a dramatical increase in the viscosity of the polymer melt due to the addition of fillers.

3.4 Effect of OC-MMT and Silatrane Loading on Mechanical Properties

Mechanical properties were measured to verify the good dispersion of silicate layers or silatrane in the polymer matrix. In this sense, tensile strength, modulus, elongation at break, impact strength and hardness of the composites were investigated and compared with the pure Nylon 12 and PVC.

(Figure 12)

(Figure 13)

The tensile strength and elongation at break of composites are illustrated in Figures 12 and 13. Initially, tensile strength gradually increased with the increase in OC-MMT loading (Lan and Pinnavaia, 1994) and became greater than that of pure polymers. This indicates that the organoclay filler can act as a reinforcement material for both Nylon 12 and PVC. After 5wt% organoclay loading, tensile strength was dropped toward higher amount of organoclay loading. The drops in tensile strength corresponds to the occurrence of stacking of silicate layers, as confirmed by WAXD diffractograms. The presence of silicate layer aggregation makes the materials to be less homogeneous and less uniform rigidity leading to the lowering of tensile strength. Considering elongation at break, it decreases largely when OC-MMT was added and further reduces largely with increasing OC-MMT content. This can be viewed as the considerable increase in rigidity of the nanocomposites. (Thajjaroen, 2000) The silicate layers were dispersed in the matrices, therefore, continuity of polymer matrix was affected by the molecular intercalation and rigidity of silicate layers. The polymeric chains are bound in the aggregate region which is lateral confined space resulting in chain extension locking in the rigid gallery region so that the molecular chains become stiff as a whole. Moreover the intercalated chain segments can be protected from the applied stress leading to strain amplification effect upon stretching. Therefore, the polymeric chains are highly stressed and broken before reaching to a regular fully oriented form, bringing about the drop in elongation at break. For a rigid polymer matrix, PVC, the tensile strengths of the nanocomposites are greater than that of pure PVC

indicating the reinforcing effect of nanocomposite structure; however, the strength gradually reduces to some steady value (about 10 MPa) with increasing OC-MMT loading. The elongation at break also reduces with increasing OC-MMT loading.

However, for Nylon12/silatrane composites, their tensile strengths were unchanged at any filler compositions within 5-20wt%. Their elongations at break drop largely to a steady value with increasing silatrane content but the values are still higher than those of Nylon12/OC-MMT nanocomposites. It could be explained that the continuous matrix was interrupted by the dispersion of silatrane. It is interesting that the drop in elongation at break of the composites reaches to the steady value since the elongations are hardly changed with silatrane loading. Both polymer composites using OC-MMT and silatrane as flame retardant sacrificed elongation property of pure polymer.

(Figure 14)

(Figure 15)

Young modulus and Hardness are shown in Figures 14-15. For the nylon 12 and PVC nanocomposites, the modulus increases sharply with the addition of OC-MMT and further increases with OC-MMT loading and likely remains steady (within the same error range) when loading is higher than 5wt%. Nylon12 has about twice less modulus than rigid PVC. The same results are found for hardness but with more obvious increasing in hardness with loading content. This suggests that OC-MMT produce nanocomposite structure that gives high rigidity.

On the other hand, Nylon12/silatrane shows increased modulus with addition of silatrane and gradually increase with increasing silatrane loading. When considering hardness, it increases with silatrane content but the increments for all loading contents are less than those of OC-MMT content. The lower modulus of silatrane suggests that silatrane are softer than OC-MMT and its spherical shape contributes less rigidity to the materials compared with sheet like structure of OC-MMT. Thus OC-MMT causing nanocomposite structure provides superior reinforcement, in term of tensile strength and modulus, to the materials over the silatrane.

(Figure 16)

In Figures 16, the impact strengths of the composites having OC-MMT and silatrane in Nylon 12 reduce about 4 (31% reduction at 9wt% loading) and 1 (11%

reduction at 20wt% loading) kJ/m^2 from the impact strength of pristine Nylon12. On the other hand, PVC/OC-MMT nanocomposites show the same impact strength as that of the pure PVC (within the error range). The slight decreased in impact strength when increasing silatrane loading suggests that spherical silatrane particles slightly interfere the mechanism of the matrix to absorb energy. For nanocomposite structure, it is interesting that the silicate layers shows different effect; i.e. in case of tough matrix (Nylon12) it reduces toughness but for the rigid matrix, it hardly influence toughness. It probably explains that the rigid matrix play more role on toughness in the low toughness region; the materials breaks according to the rigid PVC matrix that cannot withstand high energy transfer. The rigidity of the silicate layers, therefore, has no influence. This indicates that loading the inorganic fillers into a polymeric material increases brittle characteristics due to the rigidity of the inorganic filler; however, the effect of rigidity may be omitted due to the low toughness nature of the matrix.

3.5 Effect of Inorganic Fillers on Nylon 12

From previous study, the mechanical properties of Nylon 12 improved until the filler concentration reached 5wt%. Thus, 5wt% filler loading is chosen as an optimum content to study the effect of another metalatrane compound, alumatrane, as flame retardant additive on Nylon 12.

(Table 1)

Comparison of the flammability and mechanical properties of Nylon 12 with 5 wt% alumatrane, 5wt% silatrane, 5wt% OC-MMT and 5wt% MMT are shown in Table 1. Nylon 12 composites with those fillers reveal that the LOI values increase while the gross heat calorific values decrease; this suggests the improvement of flame retardation properties of these materials. The flame retardation of this system was improved possibly due to the following two reasons proposed in the literature. The first one is a reduction in the transport rate of the thermal degradation products by dramatically increasing the viscosity of the polymer melt due to the addition of the fillers. Second is the reduction in thermal diffusivity of the sample near the surface due to gradual accumulation of char formation, which acts as a thermal insulator layer (Kashiwagi *et al.*, 1999).

Mechanical properties of Nylon 12/organoclay composites in Table 1 indicate that adding organoclay into a polymeric materials increases tensile properties, but the materials become more brittle due to the intercalation of polymeric chains making more bound chains and rigidity of organoclay layer while the mechanical properties of Nylon 12/metalatrane composites was not affected. However, both inorganic flame retardants have major influenced on reducing the elongation at break.

4. CONCLUSION

In this work, we have investigated for the first time organoclay nanocomposites, silatrane and alumatrane for Nylon 12 as flame retardant materials. Alumatrane and silatrane were synthesized via the OOPS process and montmorillonite was organically modified by octadecylamine. TGA, FTIR and WAXD indicated the incorporation of OC into MMT structure. All of polymer composites were prepared via a melt blending process. The WAXD diffractograms were correlated with the TEM and SEM results showing the good incorporation of inorganic additives into polymer matrix. The exfoliated Nylon 12 and PVC/organoclay nanocomposites films are found at low OC-MMT loading. At high OC-MMT content (>5wt%), the nanocomposites became partially intercalated. Silatrane also showed good dispersion in Nylon 12 even at high composition of 20wt% as seen by SEM. The improvement in LOI values and gross heat calorific values of Nylon 12, PVC/organoclay nanocomposites and Nylon 12/metalatrane composites was observed. The general mechanism of those composites is a high performance carbonaceous silicate char built up on the surface during burning; this insulates the underlying polymer material because the char has low thermal conductivity. These composite structures appear to enhance the performance of the char through reinforcement of this char layer. Tensile strength and modulus were improved with the organophilic organoclay content up to 5wt% while unchanged with metalatrane composites. However, adding more organoclay induced brittleness.

ACKNOWLEDGEMENT

The authors would like to thank ADB Fund, King Mongkut's Institute of Technology Ladkrabang for supporting of materials, Brabender twin-screw extrusion

and Bomb calorimeter, respectively, and Assoc. Prof. Amorn Petchsom at Chulalongkorn University for the use of the LOI tester.

REFERENCES

- Blumstein, A., Parikh, K.K., and Malhotra, S.L. (1971). Influence of the nature of the exchangeable ion on the tacticity of insertion poly(methyl methacrylate). Journal of Polymer Science Part A, 1681-1691.
- Bolf, A., Jones, P., Lichtenhan, J.D., Kashiwaki, T., Lomakin, S.M., Gilman, J.W., and Harris, R.H. (1999). Additives and Modifiers for Polymers. London: Blackwell Scientific.
- Bourbigot, S., Devaux, E., and Flambard, X. (2002). Flammability of polyamide-6/clay hybrid nanocomposite textiles. Polymer Degradation and Stability, 75 (2), 397-402.
- Burside, S.D., and Giannelis, E.P. (1995). Synthesis and properties of new poly(dimethylsiloxane) nanocomposites. Chemistry of Materials, 7(9), 1597-1600.
- Carrado, K.A. (2000). Synthetic organo- and polymer-clays: preparation, characterization, and materials applications. Applied Clay Science, 17(1-2), 1-23.
- Giannelis, E.P. (1996). Polymer layered silicate nanocomposites. Advanced Materials, 8(1), 29-35.
- Gilman, J.W., and Kashiwagi, T. (1997). Nanocomposites: A Revolutionary New Flame Retardant Approach. 42nd International SAMPE Symposium, 1077-1089.
- Kashiwaki, T., and Gilman, J.W., Harris, R.H., and Nyden, M.R. (1999). Flame Retardant Mechanism of Silica. New Flame Retardants Consortium (Final Report) National Institute of Standard and Technology, 1049-1062.
- Kojima, Y., Usuki, A., Kawasumi, M., Okada, A., Kurauchi, T., and Kamigaito, O. (1993). One-pot synthesis of nylon 6-clay hybrid. Journal of Polymer Science: Part A: Polymer Chemistry, 31, 1755-1758.
- Lan, T., and Pinnavaia, T.J. (1994). Clay-reinforced epoxy nanocomposites. Chemistry of Materials, 6(12), 2216-2219.

- Lee, C.D., and Jang, W.L. (1997). Characterization of epoxy-clay hybrid composite prepared by emulsion polymerization. Journal of Applied Polymer Science, 68, 1997-2005.
- Magaraphan, R., Lilayuthalert, W., Sirivat, A., and Schwank, J.W. (2001). Preparation, structure, properties and thermal behavior of rigid-rod polyimide/montmorillonite nanocomposites. Composites Science and Technology, 61(9), 1253-1264.
- Messersmith, P.B., and Giannelis, E.P. (1995). Synthesis and barrier properties of poly(ϵ -caprolactone)-layered silicate nanocomposites. Journal of Polymer Science: Part A: Polymer Chemistry, 33(x), 1047-1057.
- Opornsawad, Y., Ksapabutr, B., Wongkasemjit, S., and Laine, R.M. (2001). Formation and structure of tris(alumatranyloxy-*i*-propyl)amine directly from $\text{Al}(\text{OH})_3$ and triisopropanolamine. European Polymer Journal, 37(9), 1877-1885.
- Thaijaroen, W. (2000). Preparation and mechanical properties of NR/clay nanocomposites. M.S. Thesis in polymer science, The Petroleum and Petrochemical College, Chulalongkorn University, Bangkok, Thailand.
- Wang, Z., and Pinnavaia, T.J. (1998). Hybrid organic-inorganic nanocomposites: exfoliation of magadiite nanolayers in an elastomeric epoxy polymer. Chemistry of Materials, 10(7), 1820-1826.
- Yang, Y., Zhu, K.Z., Yin, J., Wang, X., and Qi, Z. (1999). Preparation and properties of hybrids of organo-soluble polyimide and montmorillonite with various chemical surface modification methods. Polymer, 40, 4407-4414.
- Yano, K., Usuki, A., Okada, A., Kurauchi, T., and Kamigaito, O. (1993). Synthesis and properties of polyimide-clay hybrid. Journal of Polymer Science: Part A: Polymer Chemistry, 31, 2493-2498.

CAPTION OF TABLE

Table 1 Effect of inorganic additive (5wt%) on flammability and mechanical properties of Nylon 12

CAPTION OF FIGURES

- Figure 1 WAXD diffractograms of (a) Na⁺-Montmorillonite (MMT) and (b) OC-MMT
- Figure 2 FTIR spectra of (a) octadecylamine, (b) Na⁺-MMT and (c) OC-MMT
- Figure 3 TGA thermograms of (a) octadecylamine, (b) Na⁺-MMT and (c) OC-MMT
- Figure 4 WAXD diffractograms of (a) Nylon 12, (b) OC-MMT and Nylon 12 nanocomposites with OC-MMT loading at (c) 1wt%, (d) 3wt%, (e) 5wt%, (f) 7wt% and (g) 9wt%
- Figure 5 WAXD diffractograms of (a) PVC, (b) OC-MMT and PVC nanocomposites with OC-MMT loading at (c) 1wt%, (d) 3wt%, (e) 5wt%, (f) 7wt% and (g) 9wt%
- Figure 6 TEM micrographs of cross-sectional of (a) Nylon 12/OC-MMT (5%wt) and (b) PVC/OC-MMT (5%wt)
- Figure 7 WAXD diffractograms of (a) Nylon 12, (b) silatrane and Nylon 12 composites with silatrane loading at (c) 5wt%, (d) 10wt%, (e) 15wt% and (f) 20wt%
- Figure 8 SEM micrographs of Nylon 12 composites with silatrane loading at (a) 5wt%, (b) 10wt%, (c) 15wt% and (d) 20wt%
- Figure 9 Effect of OC-MMT and silatrane loading on LOI value of Nylon 12 and PVC
- Figure 10 Effect of OC-MMT and silatrane loading on the gross heat calorific value of Nylon 12 and PVC
- Figure 11 The char formation at polymer surface of (a) Nylon 12/OC-MMT, (b) PVC/OC-MMT and (c) Nylon 12/silatrane
- Figure 12 Effect of OC-MMT and silatrane loading on tensile strength of Nylon 12 and PVC
- Figure 13 Effect of OC-MMT and silatrane loading on elongation at break of Nylon 12 and PVC
- Figure 14 Effect of OC-MMT and silatrane loading on modulus of Nylon 12 and PVC

Figure 15 Effect of OC-MMT and silatrane loading on hardness (Shore D) of Nylon 12 and PVC

Figure 16 Effect of OC-MMT and silatrane loading on impact strength of Nylon 12 and PVC

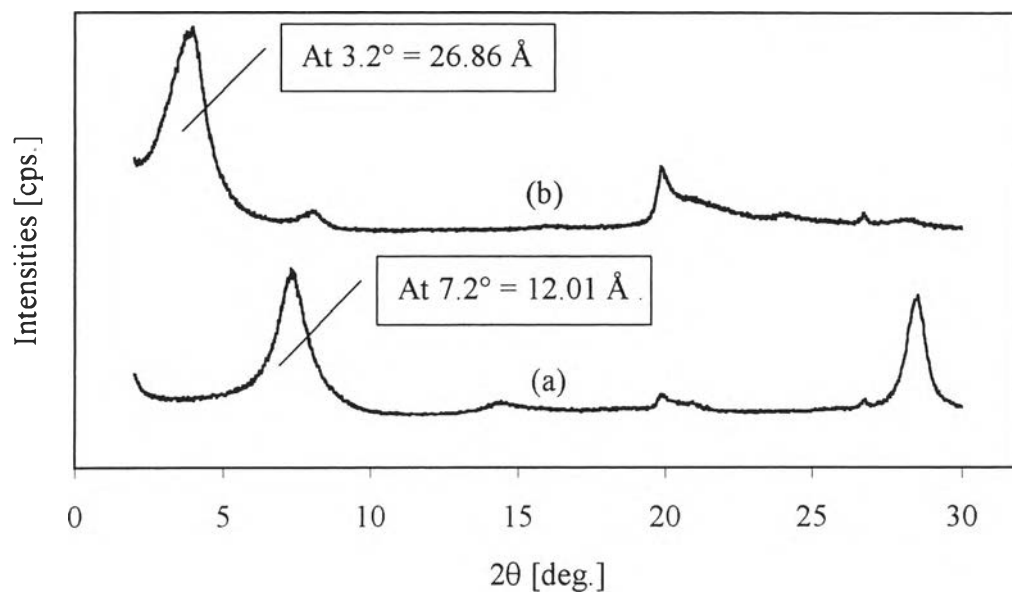


Figure 1

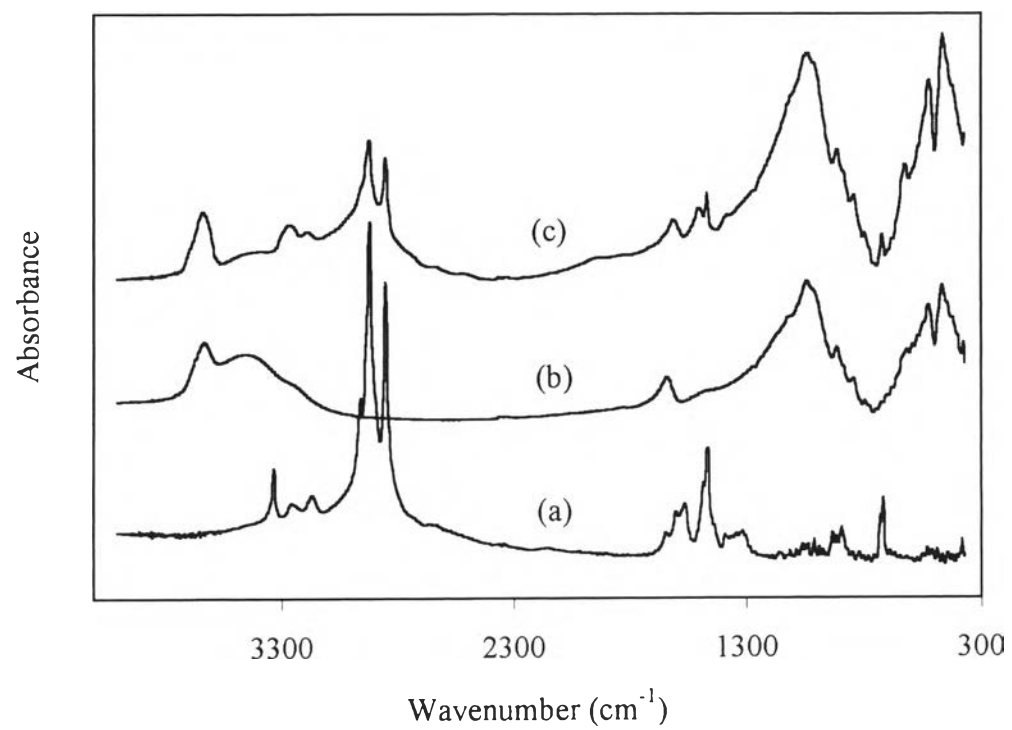


Figure 2

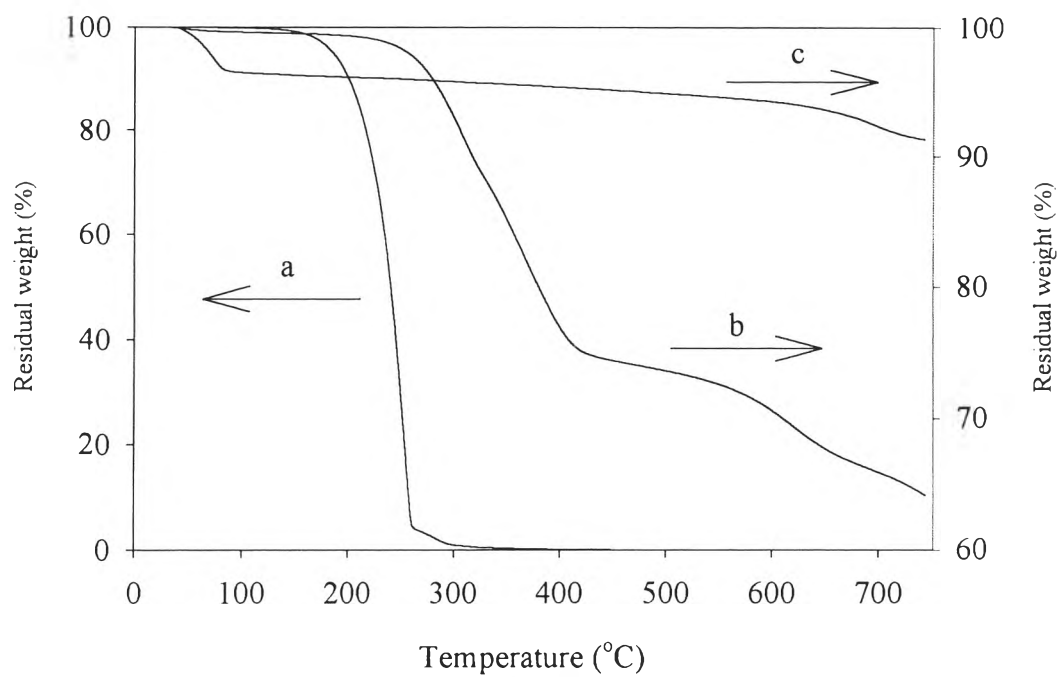


Figure 3

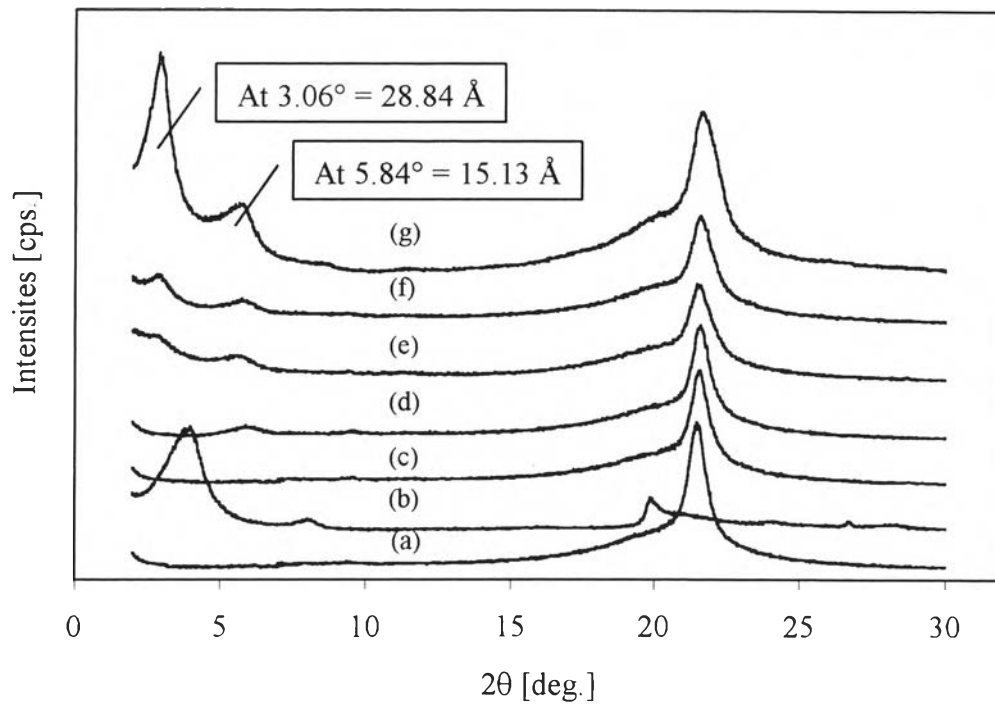


Figure 4

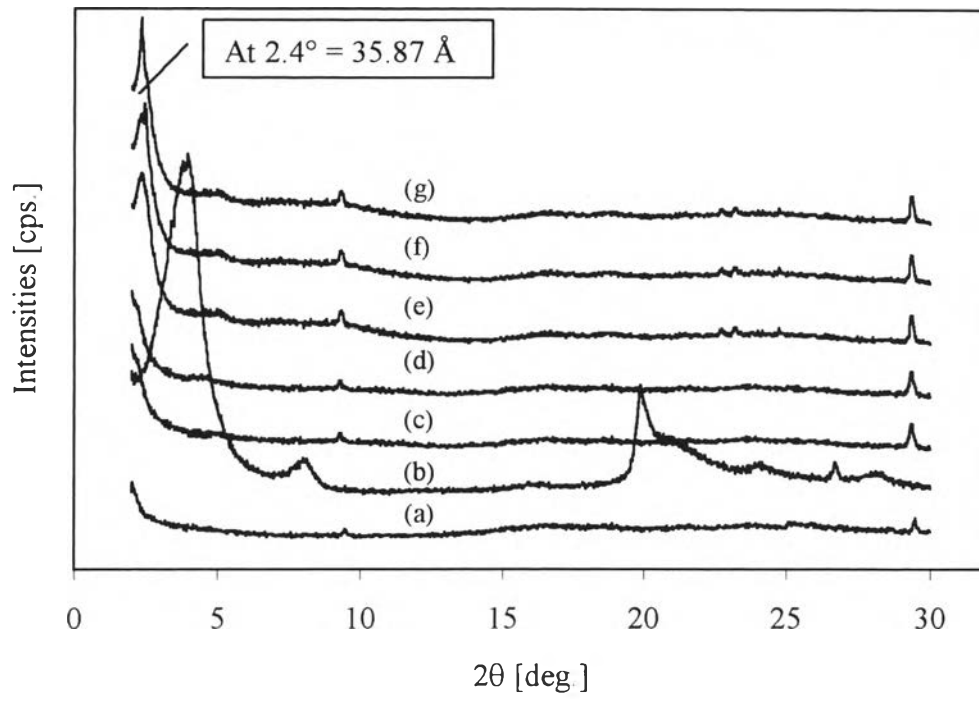


Figure 5

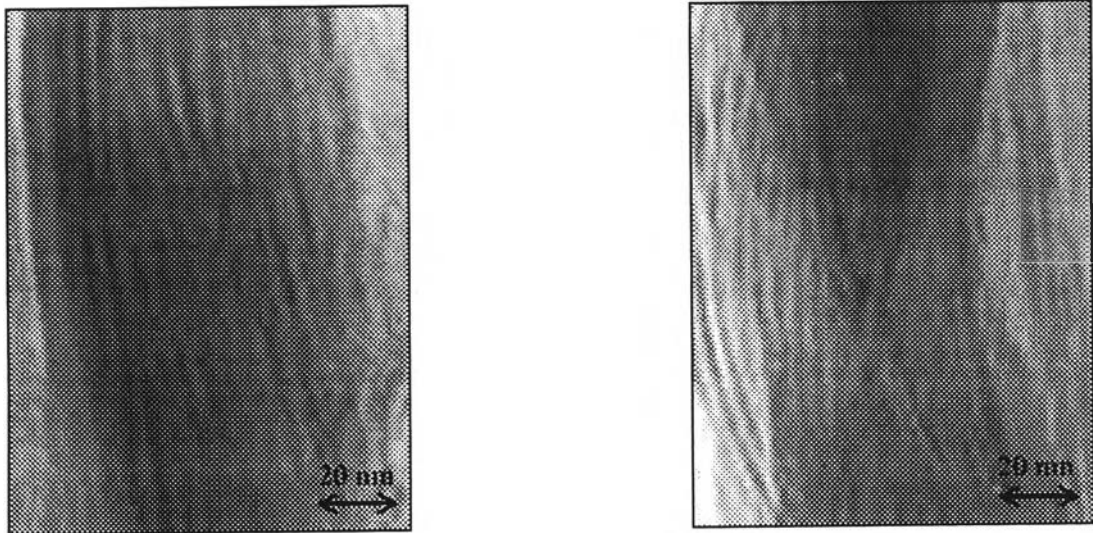


Figure 6

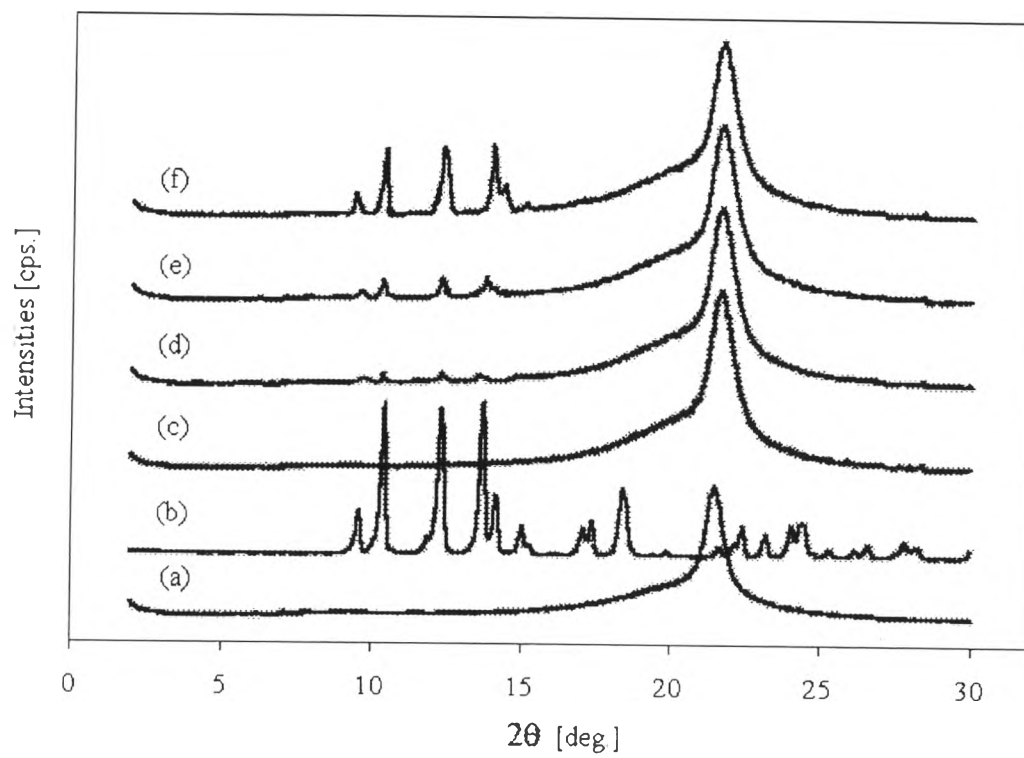


Figure 7

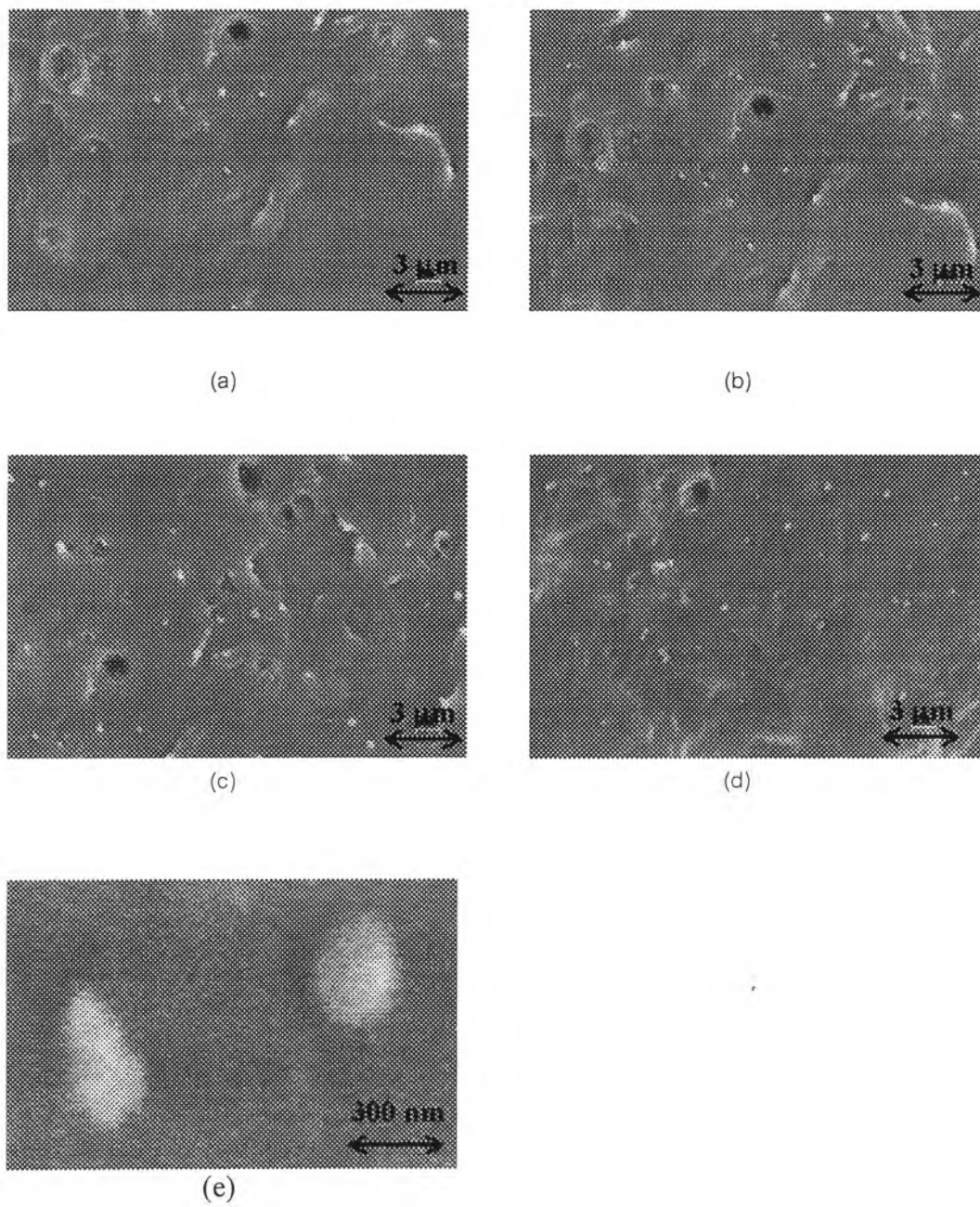


Figure 8

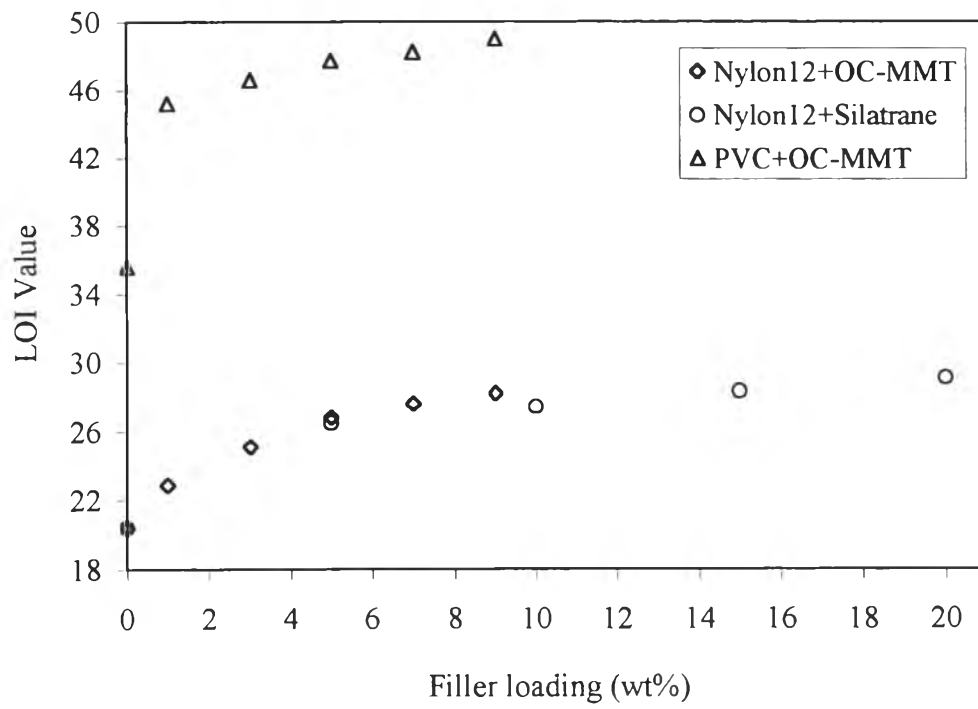


Figure 9

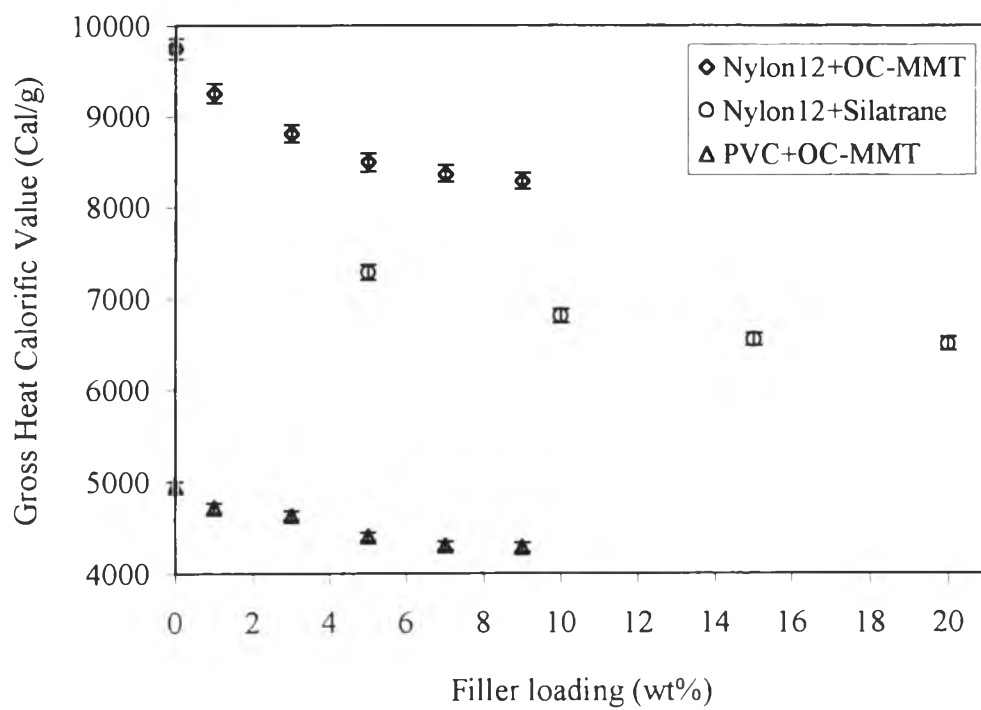
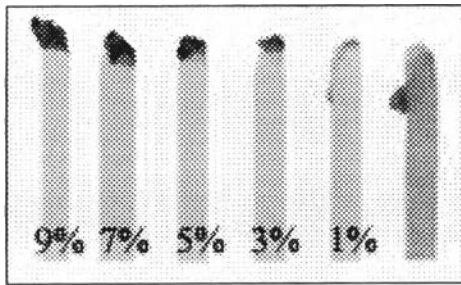
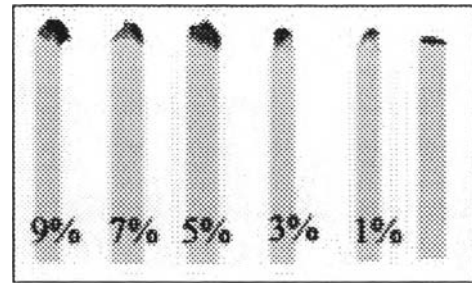


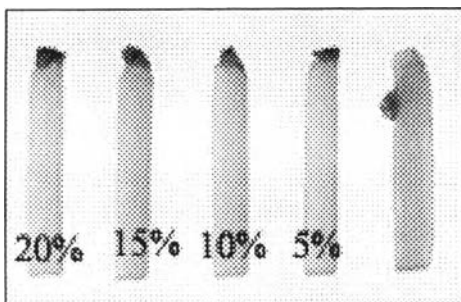
Figure 10



(a)



(b)



(c)

Figure 11

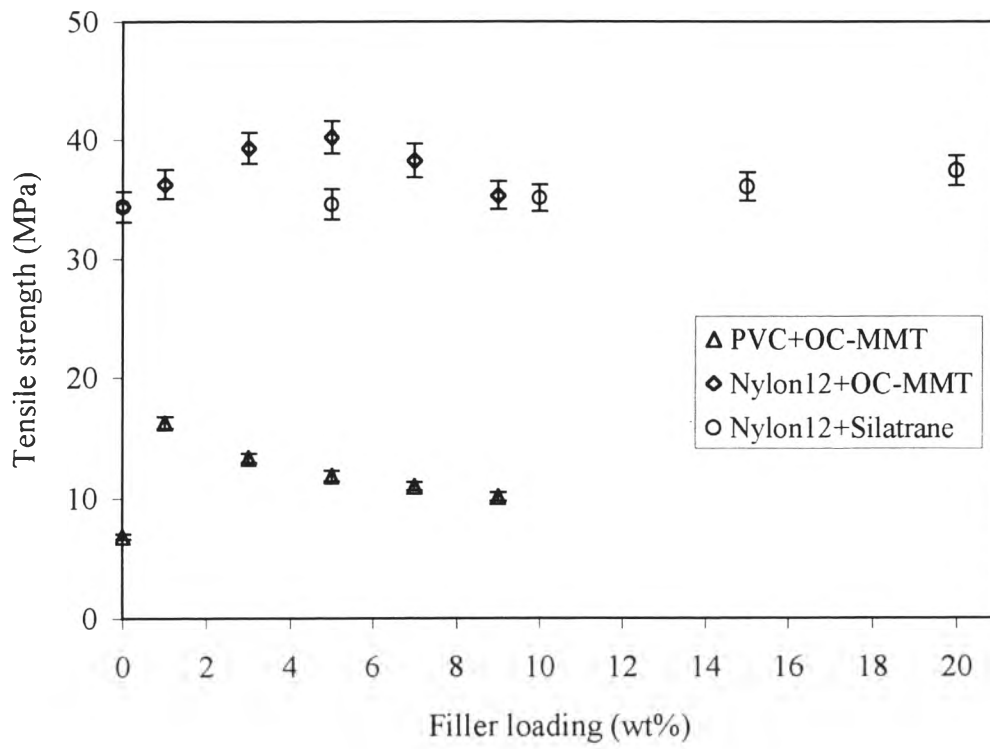


Figure 12

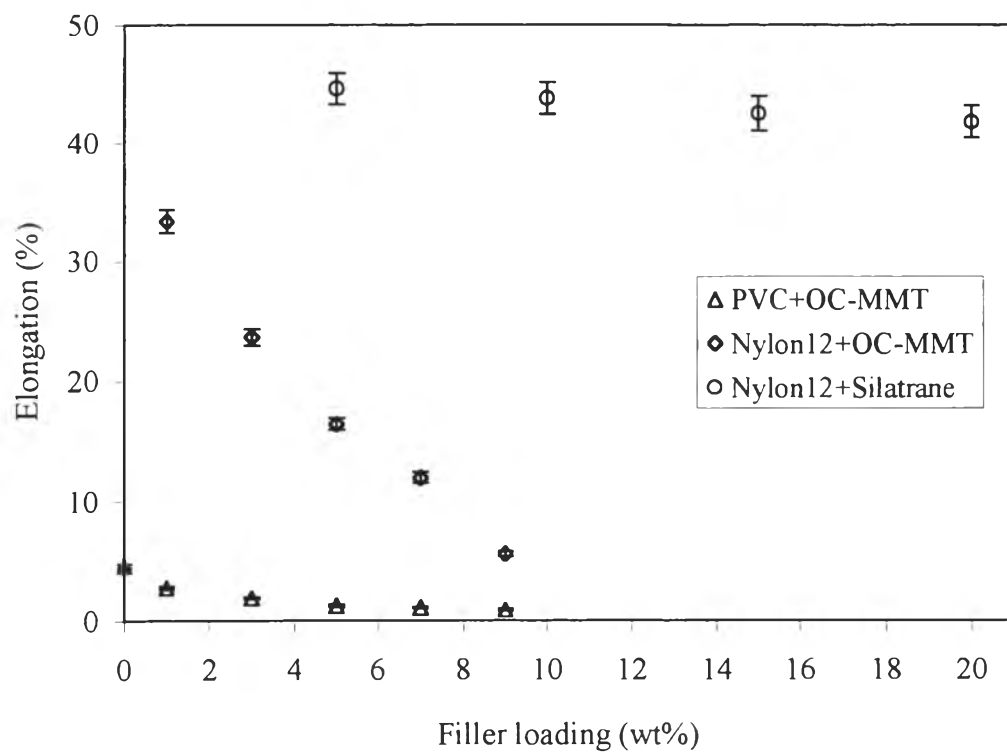


Figure 13

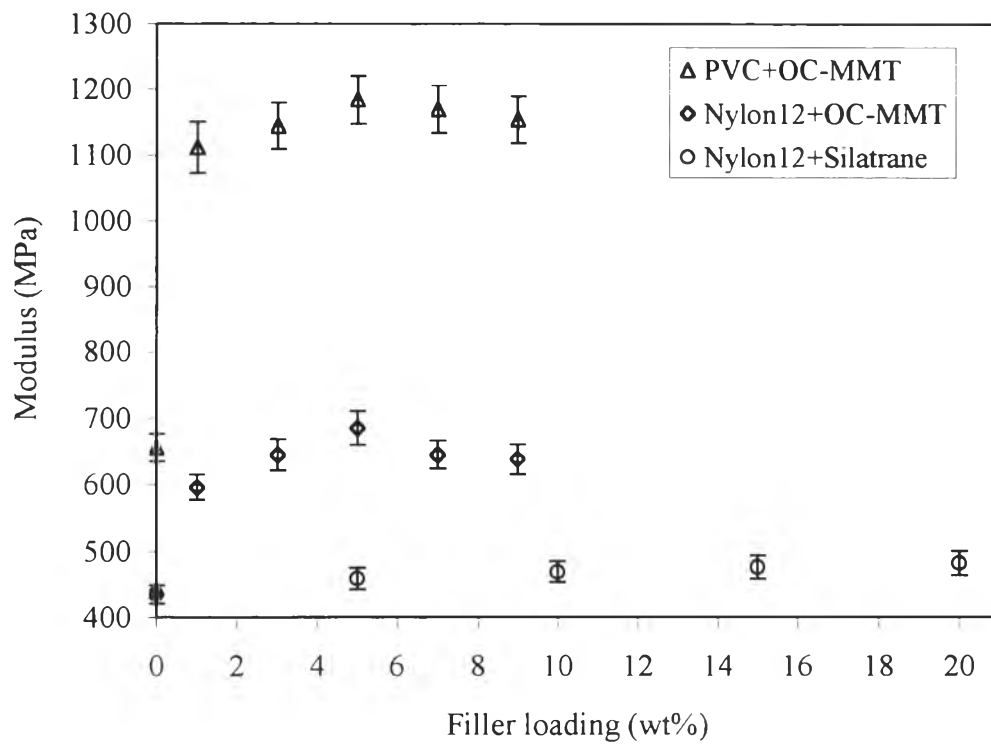


Figure 14

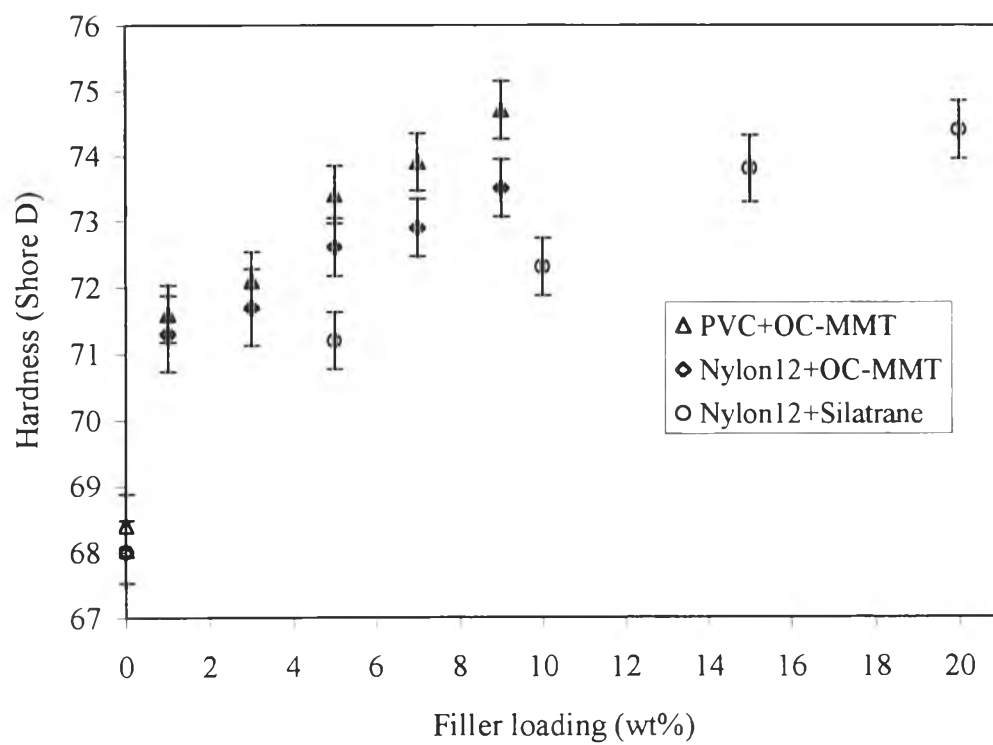


Figure 15

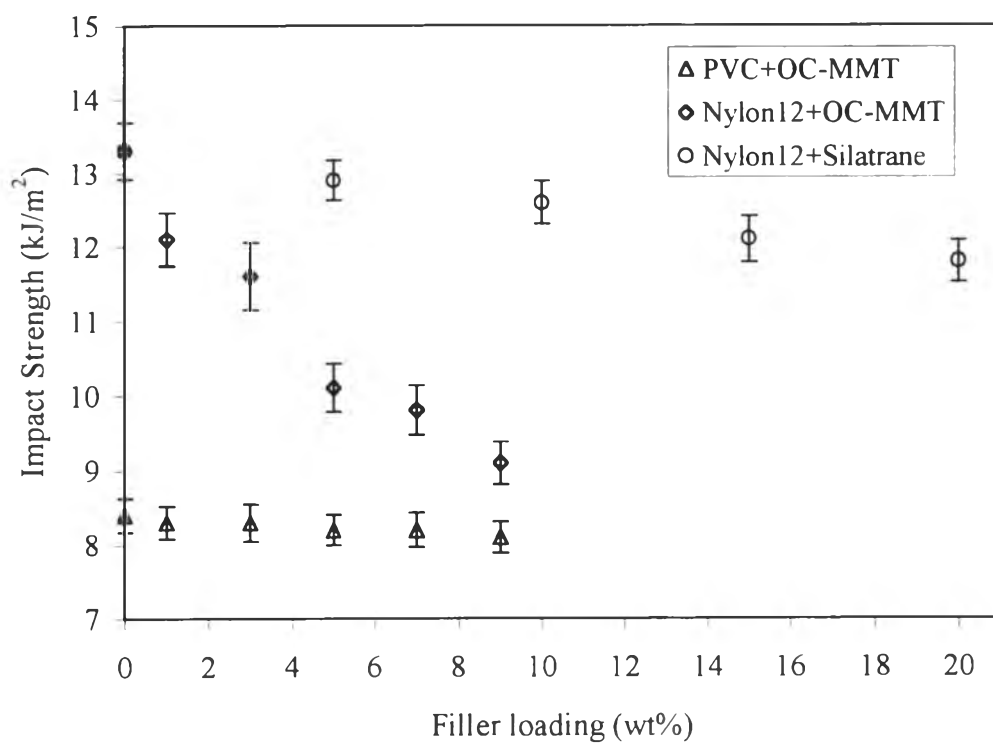


Figure 16

Table 1 Effect of inorganic additives (5wt%) on flammability and mechanical properties of Nylon 12

Nylon12 composites	Properties						
	LOI value	Gross Heat Calorific (cal/g)	Tensile Strength (MPa)	Modulus (MPa)	Elongation at break (%)	Impact strength (kJ/m ²)	Hardness (Shore D)
pure Nylon12	20.4	9743.61	34.4	435.2	301.4	13.3	68
Nylon12/alumatrane	26.4	7288.32	35.3	459.9	43.2	12.8	71
Nylon12/silatrane	26.5	7285.64	34.6	458.7	44.6	12.9	71
Nylon12/OC-MMT	26.8	8493.51	40.3	685.3	16.4	10.1	73
Nylon12/MMT	25.4	8304.25	34.2	548.0	9.0	9.5	73